Sizing and optimization of a more electric aircraft integrating short-term incremental technologies

Thomas Planès, Scott Delbecq, Valérie Pommier-Budinger, Valérian Palanque, Emmanuel Bénard

33RD CONGRESS
OF THE INTERNATIONAL COUNCIL
OF THE AERONAUTICAL SCIENCES
STOCKHOLM, SWEDEN, 4-9 SEPTEMBER, 2022

ICAS 2022 SWEDEN

SIZING AND OPTIMIZATION OF A MORE ELECTRIC AIRCRAFT INTEGRATING SHORT-TERM INCREMENTAL TECHNOLOGIES

Thomas Planès[1], Scott Delbecq[1], Valérie Pommier-Budinger[1], Valérian Palanque[1,2] & Emmanuel Bénard[1]

[1]ISAE-SUPAERO, Université de Toulouse, France
[2]ONERA/MFE, Université de Toulouse, France

Abstract

In order to reduce the environmental impact of aviation, one of the solutions is to develop more efficient aircraft. These gains can be achieved in different fields such as propulsion, aerodynamics or electrification of systems. This paper focuses on the sizing and optimization of BEITA, a short-medium range aircraft architecture available in the short term by 2025-2030. The aircraft is based on incremental technologies for propulsion, aerostructure and bleedless systems. Light-weight models are proposed for the different improvements, particularly for more electric systems. FAST-OAD, an open source framework for rapid overall aircraft design based on multidisciplinary design analysis and optimization, is used to size the new architecture and a specific life cycle assessment module is used to estimate the environmental impacts. BEITA allows a reduction in fuel consumption of 15% compared to the CeRAS reference aircraft. Optimizations of this architecture are achieved minimizing different cost functions. This study ends with a sizing on a shorter range based on specific payload-range diagrams.

Keywords: Overall Aircraft Design, Aircraft systems, MDAO, FAST-OAD, Life Cycle Assessment

Nomenclature

AWG	American Wire Gauge
BEITA	Bleedless and Efficient Incremental Technologies Aircraft
CeRAS	Central Reference Aircraft data System
ECS	Environmental Control System
FAST-OAD	Future Aircraft Sizing Tool - Overall Aircraft Design
IPS	Ice Protection System
LCA	Life Cycle Assessment
LWC	Liquid Water Content
MDAO	Multidisciplinary Design Analysis and Optimization
MTOW	Maximum Take-Off Weight
OAD	Overall Aircraft Design
OWE	Operating Empty Weight
RPK	Revenue Passenger Kilometer
SFC	Specific Fuel Consumption
TLAR	Top Level Aircraft Requirement
UHBR	Ultra-High Bypass Ratio

1. Introduction

Environmental issues are becoming increasingly important in public and scientific debates, and call for a transition to a sustainable society. One of the major issues is climate change, which requires a quick reduction in greenhouse gas emissions. In this context, aviation currently represents between 2 and 3% of CO_2 emissions, to which must be added non-CO_2 climate impacts such as condensation trails [1]. Recent studies have focused on transition scenarios specific to aviation, using various levers of action available such as technological improvements or evolution of the air traffic level [2, 3, 4].

Technological levers of action to reduce CO_2 emissions are particularly studied in the literature. In general, two types of improvement are studied [5]. On the one hand, the replacement of fossil kerosene is considered. The energy carriers commonly studied are electricity (stored in batteries) [6], hydrogen [7], biofuel [8, 9] and electrofuel [10]. On the other hand, improving the energy efficiency of the aircraft is the other solution to reduce CO_2 emissions by minimizing energy consumption [11]. It can be achieved enhancing for example operations, propulsion, aerodynamics or systems.

For these latter, there are many examples of recent and new technologies being considered to improve aircraft efficiency, particularly in terms of more electric aircraft [12] and system integration [13, 14, 15]. For instance, electric bleedless systems are studied to replace conventional architectures for environmental control system (ECS) [16]. Similarly, electric ice protection system (IPS), based on thermal-electric [17] or electro-mechanical [18, 19] solutions, are studied in replacement of conventional IPS using pneumatic boots or hot air from engines [20, 21]. Moreover, the increase of electrical power due to these new systems will strengthen the burden put on the thermal management system which mainly relies on fuel as heat drain [22]. Hence, such system is prone to become an even more critical and complex system.

More generally, many works are interested in the complete evaluation of new aircraft architectures. First of all, there are articles about new concepts in regional aviation. Indeed, hydrogen architectures with a design range of 200 NM and hybrid propulsion are studied in [23] whereas all-electric and hybrid-electric architectures with a design range of 300 km are treated in [24, 25]. Studies are also carried out on commercial aircraft with larger range. For architectures with partial or full electrification of the propulsion, results are conflicting. Some studies conclude that electric propulsion is not a promising path to significant reduction of emissions before 2050 [26], whereas others estimate that all-electric aircraft have the potential for lower emissions [27]. Finally, disruptive aerodynamic and structural architectures are studied. Blended wing body architectures would allow consumption gains of about 25% [28] while turboelectric aircraft with boundary layer ingestion could reduce fuel consumption by 7% [29].

Some limitations can be noted on these different studies. Firstly, some studies only consider a specific system and the impacts on the aircraft architecture are not taken into account, as in the case of the integration of more electric non propulsive systems. Secondly, most studies focus on breakthrough architectures, particularly based on new propulsion systems, which are not yet mature. These will be necessary to achieve low-carbon aviation, but do not address the issue of reducing emissions in the short term. Lastly, when sizing systems or complete architectures, the choice of the minimization objective varies and is not always specified. If the impact of the mass is often considered, its minimization does not always allow reaching the optimum in terms of reducing the climate impact, in particular in the case of more electric systems.

As a consequence, this paper proposes to address the sizing and optimization of a more electric aircraft for hypothetical entry into service by 2025-2030 integrating incremental technologies available at short term for propulsion, aerostructure and non-propulsive systems. This study includes a complete analysis of the aircraft thanks to an overall aircraft design framework. Different optimization objectives are considered to evaluate their advantages and drawbacks and deduce their relevance.

To this end, the paper is organized as follows. In section 2. the different methods used in this paper are detailed. A particular attention is given to the overall aircraft design framework FAST-OAD and its use to size an aircraft architecture. Then, section 3. presents the reference aircraft and the technological improvements considered in this paper. The corresponding models added to FAST-OAD are synthesized in section 4. Aircraft sizing and optimization is achieved in section 5. for different relevant objectives. Lastly, section 6. offers concluding remarks.

2. Methods and tools

This section introduces the different methods and tools useful for the paper. The overall aircraft design framework FAST-OAD is presented as well as a specific LCA method. The procedure for sizing and optimizing aircraft architectures is detailed.

2.1 Presentation of FAST-OAD

Overall aircraft design tools allow sizing and optimizing an aircraft for a given set of specifications by integrating various disciplines. These frameworks often rely on Multidisciplinary Design Analysis (MDA) and Optimization (MDO) techniques. These latter allow performing optimizations of systems that depend on a large number of disciplines and that include multidisciplinary couplings (algebraic loops). The study of aeronautical systems requires in most cases this approach during the design and optimization phases. The optimization problem includes an objective, variables and constraints present in the different disciplines of aircraft design. To perform the optimizations, different MDO formulations and techniques can be used [30, 31, 32].
In this paper, the FAST-OAD framework, based on OpenMDAO [33], is considered and detailed in [34]. This tool focuses on CS-25/FAR-25 category aircraft. The overall aircraft design process is given on Figure 1. Major modules can be detailed: geometry, weight, aerodynamics, propulsion and performance.

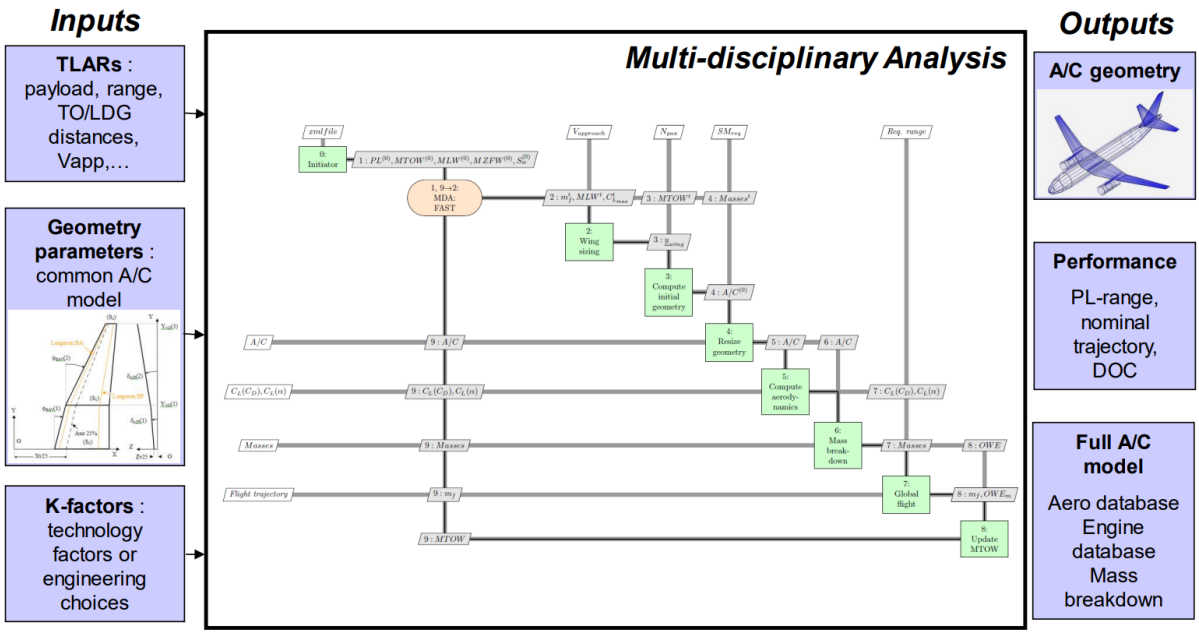

Figure 1 – FAST-OAD overall architecture [34].

However, this tool has several limitations which offer development perspectives. First, aircraft systems are only included using correction coefficients on the global architecture. As a consequence, the relevance of replacing conventional systems through electrification is difficult to assess. Then, the turbofan models remain relatively simple and are adapted to old generation engines. Lastly, this framework is limited to traditional tube and wing aircraft architectures.

2.2 Life Cycle Assessment module

For evaluating the environmental performance of the aircraft, a specific LCA module, developed in [35], is used in addition to FAST-OAD. Designed for being used with overall aircraft design frameworks, it allows sizing architectures that minimize the climate impact of the aircraft.
The specific methodology and models are detailed in [35]. In a synthetic way, the inventory for emissions and resources is made using EcoInvent database and open-source aircraft data for emission factors. The life cycle includes aircraft production, airport use, fuel production and fuel consumption during the flight. The LCA method to estimate the environmental impacts is ReCiPe 2016 [36].

It is interesting to note that the non-CO_2 climate effects such as contrails are not included in this module, which focuses on usual greenhouse gases. Indeed, taking them into account for a single aircraft is complex. Recent work has focused on how to quantify these effects for single flight [37].

2.3 Sizing and optimization procedure

This section describes the sizing and optimization procedure implemented in the paper to obtain results on the impact of short-term technology improvements and the choice of optimization goals.
This procedure relies on FAST-OAD to perform an MDAO of the overall aircraft design process. To scale more efficient architectures, FAST-OAD will be supplemented to add updated or new models. For systems benefiting from a simple technological improvement, correction factors are sufficient to update the model. For new systems, specific models must be developed and integrated. Lightweight models such as scaling laws or substitution models based on dimensional analysis [38] are sought to reduce the number of parameters and facilitate the convergence of calculations. For the optimization, some aircraft parameters will be considered as variables and the aircraft constraints will be taken into account. Different objective functions will be studied which will lead to different optimized aircraft. Finally, starting from the results of the MDAO, the LCA module is used to evaluate the architecture of the optimized aircraft in terms of environmental impact.

3. Presentation of the aircraft architectures studied

The objective of this section is to present the reference aircraft as well as the new aircraft configuration studied resulting from the different improvements considered.
The CeRAS (Central Reference Aircraft data System) aircraft is a basic aircraft used in order to validate aircraft models [39]. The Top Level Aircraft Requirements (TLARs) of this aircraft are in given in Table 1. CeRAS is considered as the reference aircraft for this study.

Table 1 – TLARs of CeRAS aircraft (calibrated for FAST-OAD).

Parameter	Value	Unit
Passenger capacity	150	PAX
Maximum payload	19.6	t
Sizing range	2500	NM
Sizing payload	17	t
Design range	2750	NM
Study range	800	NM
Design/Study payload	13.6	t
Cruise Mach number	0.78	-
Reserves - Diversion distance	200	NM
Reserves - Holding duration	45	min

The aircraft sized and optimized in this paper is a more electric architecture, available by 2025-2030, integrating short-term incremental technologies. The sizing is based on the same TLARs as CeRAS as well as on the same geometrical characteristics. This aircraft incorporates a more efficient propulsion system, an improved aero-structure and more electric systems.
In terms of propulsion, ultra-high bypass ratio engines (UHBR) are expected at short term to replace the more recent turbofan. A change in aspect ratio is envisaged in order to improve aerodynamic performance. For the structure, a mass reduction is assumed thanks to an increasing use of composite materials and improvements in manufacturing processes. For the systems, electric bleedless systems are integrated. As a consequence, an electro-thermal system is used for IPS and an electric ECS is considered inspired by Boeing 787 architecture. However, the integration of electric systems imposes constraints that influence the sizing and require additional systems, for instance at the electric and thermal level [40]. As a consequence, power generation and distribution systems are considered to also provide energy to bleedless systems and thermal management systems are used in order to cool electric systems.

4. Technologies modeling

This section presents the method used for the different technologies. However, it is not the objective to describe the models in detail. Different approaches are used in this paper. For instance, models for bleedless systems are specifically developed and integrated in FAST-OAD, while propulsion models are based on correction coefficients applied to classical models available in FAST-OAD.

4.1 Propulsion, aerodynamics and structure

In this section, the models dedicated to propulsion, aerodynamics and structure are synthesized.
For the turbofan, an UHBR engine is assumed to be available. Indeed, this solution is studied in the scientific literature [41] and in the industry. For estimating the performance of the new turbofan, the rubber engine model from FAST-OAD [42] is considered, assuming a maximum Mach number of 0.85. Based on engine data tables, it allows modeling the turbofan with a set of variables, like for instance the bypass ratio. Correction factors are used to correct the specific fuel consumption (SFC) obtained but also the engine mass. The parameters for different engines of single-aisle aircraft are given for comparison in Table 2. IAE-V2527-A5 (reference engine of CeRAS), CFM-56-5B and CFM-LEAP-1A parameters have been set up in order to match with industrial data, whereas UHBR parameters have been tuned in order to reduce cruise SFC by 20% in comparison to CeRAS engines and match LEAP-1A mass by removing bleed air system and considering a shorter bypass nozzle.

Table 2 – FAST-OAD parameters for IAE-V2527-A5, CFM-56-5B, LEAP-1A and UHBR engines.

Parameter	**IAE-V2527-A5**	**CFM-56-5B**	**LEAP-1A**	**UHBR**	**Unit**
Bypass ratio	4.9	5.5	11	15	-
Overall pressure ratio	32.6	34.4	40	45	-
Turbine inlet temperature	1633	1633	1833	1933	K
Maximum take-off thrust	118	133	143	150	kN
Design altitude	33000	33000	34500	34500	ft
Correction factor for take-off SFC	0.83	0.83	1.14	1.66	-
Correction factor for cruise SFC	1.03	0.96	0.95	0.85	-
Correction factor for engine mass	1.00	0.96	1.12	1.08	-
Results	**IAE-V2527-A5**	**CFM-56-5B**	**LEAP-1A**	**UHBR**	**Unit**
SFC at maximum take-off	10.0	9.6	9.3	9.0	g/s/kN
SFC at cruise bucket point	16.7	15.4	14.4	13.5	g/s/kN
Engine mass	2360	2480	3050	3050	kg

Aerodynamic improvements are only considered modifying the aspect ratio. For the structure, a 5% mass reduction is assumed for fuselage, wing and tails using correction factors. In both cases, classical models from FAST-OAD are used and no new model is needed.

4.2 Electric bleedless systems

In order to remove bleed air system from engines, electric bleedless systems are considered for ECS and IPS. Dedicated models are described in this section.

4.2.1 Environmental Control System

ECS is the most consuming aircraft system and allows achieving multiple functions such as heating or cooling of the cabin, air renewal and pressurization. Conventional systems are based on taking air from the turbofan which is then brought to the correct temperature and pressure conditions in the cabin. The objective is to electrify this system to make the architecture bleedless.
The architecture studied is presented on Figure 2. Taken directly from the outside via air inlets, air is compressed and therefore heated via an electrically-operated compressor. Then, the air passes through a first exchanger (cooled by outside air) to decrease the temperature and in a second compressor. Subsequently, the air goes through a second exchanger and through a turbine for expansion. Finally, this air can be mixed with recirculated air from the cabin to reduce the mass flow taken from the ram air. The objective is to reach the right level of temperature and pressure.

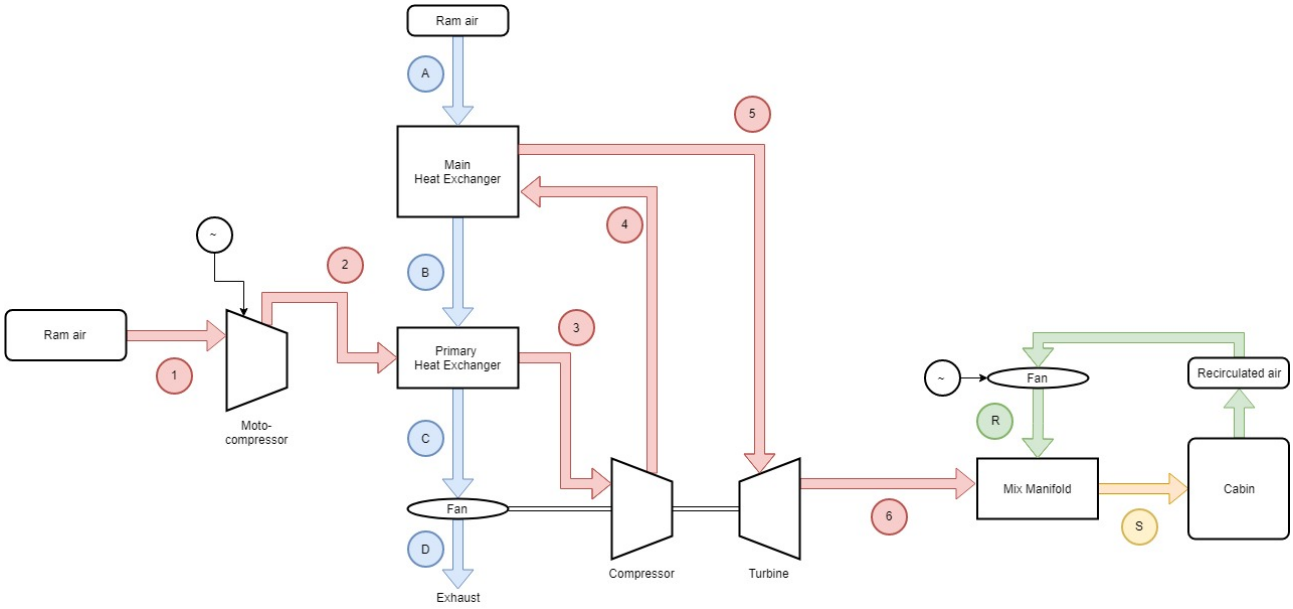

Figure 2 – Diagram of the ECS architecture studied.

At system level, several characteristics to ensure the main functions of the ECS can be calculated [13]. For instance, heat loads HL, depending on different terms given in equation (1), allows knowing the requirements in terms of cabin heating or cooling. HL_{ext} are the external thermal loads due to convection heat transfer, HL_{pax} the metabolic thermal loads due to passengers, HL_{solar} the solar loads and HL_{elec} the electric loads.

$$HL = HL_{ext} + HL_{pax} + HL_{solar} + HL_{elec} \tag{1}$$

These different characteristics allow estimating required air flows to ensure a function. For instance, in the case of a cooling with estimated heat loads HL, the required mass flow rate $\dot{m}_{cooling}$ can be estimated using equation (2), with C_p the specific heat capacity, T_{cab} the cabin temperature and T_s the blown air temperature. The maximum mass flow rate, called Flow Schedule, is used to size the system.

$$\dot{m}_{cooling} = \frac{HL}{C_p(T_{cab} - T_s)} \tag{2}$$

At component level, cross-flow plate fin type heat exchangers are considered and modeled using NTU method [43]. For turbomachines (compressor, turbine, fan), Cordier diagram [44] and scaling laws are used. The first one allows linking two sizing parameters of a turbomachine when the second one, often used in actuator sizing [45], allows studying the effects of a geometric change on the characteristics of a ”custom-made” component compared to an existing reference component. Concerning electric motors, scaling laws are also used assuming that the cooling of the motors are included in the models. Then, air inlets models are similar to those used for thermal management system in section 4.3.2 Lastly, thermodynamics models allow linking the different components in terms of temperature, pressure and mass flow. Isentropic transformations associated with isentropic efficiencies are assumed.
The methodology allows modeling accurately all ECS characteristics for different sizing points. Nevertheless, its direct integration into aircraft design tools such as FAST-OAD is too complex without reducing models into surrogate models. Indeed, the ECS design optimization problem includes 24 design variables and 42 constraints. Therefore, in this work, ECS has been sized separately considering only TLARs and main characteristics such as the fuselage size, which have been assumed using CeRAS data. The results obtained for ECS (mass, mean and maximum drag, mean and maximal electric power consumption) have been directly integrated into the sizing of the aircraft architecture.

4.2.2 Ice Protection System

IPS is along with ECS the other pneumatic system that can be found in some aircraft. Conventional thermal pneumatic IPS uses heated air taken from the engines and distributes it along the surfaces to be protected. IPS is not often used during the flight, but the sizing of IPS implies constraints in terms of power consumption. For single-aisle aircraft, wing and nacelles are protected against ice using a specific system, which can perform anti-icing (preventing ice from forming) or de-icing (removing ice already formed) functions. A surface may be anti-iced by heating to a temperature that evaporates water upon impingement (evaporative protection), or by heating the surface just enough to prevent freezing (running-wet protection). Similarly to ECS, the objective is to electrify this system.
The architecture studied is based on thermal-electric systems using heating mats [46]. For pod protection, an anti-icing system with a running-wet protection is considered. This protection prevents the formation of ice which can be dangerous for the engines. For wing protection, a de-icing system may be considered in order to reduce the power consumption of the system. The wing IPS is presented on Figure 3. It is divided into parting strips, which operate continuously to ensure a local running-wet anti-icing, and other areas where the heating mats are activated sequentially and cyclically in order to de-ice locally.

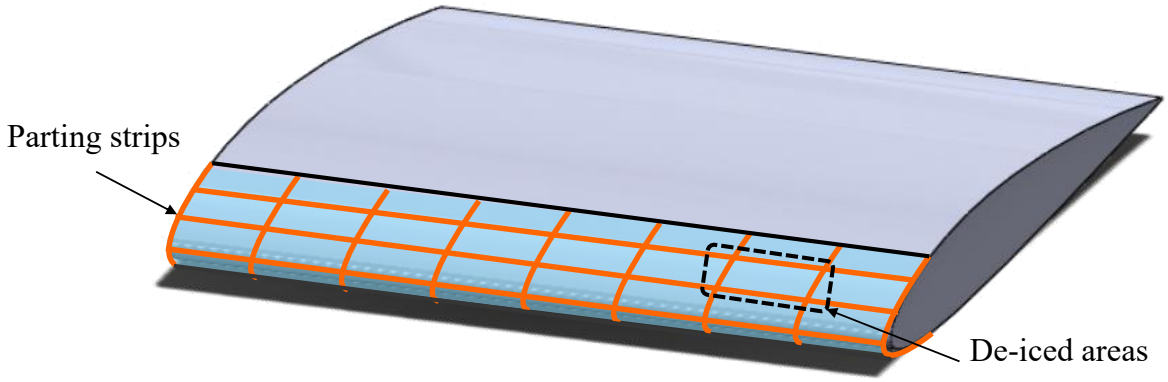

Figure 3 – Schematic architecture of wing IPS.

In this paper, only wing IPS models are presented, but the method can be easily adapted for pod IPS. At system level, it is necessary to estimate the power requirements for protecting the wing. This estimation depends on the power required to fulfill a running-wet anti-icing function on parting strip areas and the power required to shed the remaining ice on other areas. According to AIR1168/4 [47], parting strips are assumed to represent around 20% of the total protected area. These powers can be estimated using different methods available in [20, 47, 48, 49]. The sizing flight point studied in this paper is at an altitude of $20,000\ ft$, an aircraft speed of $154\ m/s$, an outside air temperature of -9°C and a Liquid Water Content (LWC) of $0.44\ g/m^3$, according to AIR1168/4.
On the one hand, the power P_A for anti-icing parting strips with a running-wet protection is given in equation (3) as a sum of different terms. Three terms are positive and increase the required power. P_{conv} is the external power due to convection heat transfer, depending on the heat transfer coefficient and the skin temperature fixed at 10°C based on AIR1168/4. P_{sens} is the sensible heat power which gives the power required to bring water to a liquid state at skin temperature. P_{evap} represents the power used to partially evaporate water. The two previous terms depend on LWC which corresponds to the water mass in a specific amount of dry air. In contrast, two terms are negative and decrease the required power. P_{aero} depends on Mach number and represents the aerodynamic effects of the flow velocity. P_{kine} represents the kinetic energy added by impinging droplets.

$$P_A = P_{conv} + P_{sens} + P_{evap} + P_{aero} + P_{kine} \tag{3}$$

On the other hand, concerning the other areas, the shedding of the remaining ice is performed by melting a thin ice layer at the ice/skin interface. Upon melting, the ice bulk is detached thanks to aerodynamic forces. In order to reduce the maximum required power, the de-iced surfaces of total area A_D are divided into independent surfaces of area $A_{D,cycled}$ where heating mats are activated cyclically. The maximum area of these independent surfaces depends on two characteristic durations. The melting duration $\Delta t_{melting}$ corresponds to the duration of heating mat operation. It is chosen to be 9 seconds as recommended by AIR1168/4, corresponding to a good trade-off between heating mat power and their associated mass. The melted layer thickness is assumed to be $0.5\ mm$ [49]. The de-icing cycle duration Δt_{cycle} corresponds to the duration between two cycles. Typical values are between 1 to 3 minutes according to AIR1168/4. A mean duration of 2 minutes is selected in this case, corresponding to a maximum ice layer thickness of 1.2 mm in the icing and flight conditions considered. The maximum area $A_{D,cycle}$ is thus calculated using equation (4).

$$A_{D,cycle} = A_D \frac{\Delta t_{melting}}{\Delta t_{cycle}} \tag{4}$$

The power P_D required to detach the ice on each independent surface can be expressed as in equation (5). m_{ice} is the mass of the melted thin ice layer on the surface $A_{D,cycle}$, T_{ref} the melting temperature of the ice, $C_{p,ice}$ the heat capacity of the ice, $\Delta H_{f,ice}$ the latent heat of fusion of water and T_{skin} the equilibrium skin temperature, computed using AIR1168/4.

$$P_D = \frac{m_{ice}}{\Delta t_{melting}} \left(C_{p,ice}(T_{ref} - T_{skin}) + \Delta H_{f,ice} \right) \tag{5}$$

As a consequence, the effective total required power P_T is obtained using equation (6) depending on heating mat efficiencies. An efficiency of $\eta_A = 0.9$ is taken for anti-iced areas, whereas a degraded efficiency of $\eta_D = 0.7$ is assumed for de-iced areas due to local and intermittent use.

$$P_T = \eta_A P_A + \eta_D P_D \tag{6}$$

At component level, many heating mat architectures are detailed in the literature [17, 50, 51, 52]. The heating mats studied here are based on AIR1168/4 and utilize glass cloth impregnated for instance with epoxy resins as dielectric material, protected by a metal cladding. The thickness is around $1.4\ mm$ and the area density of this component is $3.7\ kg/m^2$.

4.3 Additional systems due to electrification

The electrification of the pneumatic systems induces some changes in other system requirements. Power generation, power distribution and thermal management are considered here. Mass and efficiency models are provided to take these systems into account.

4.3.1 Power generation and distribution systems

For power generation, electric generators and power inverters are studied. The modeling is based on simple coefficients extracted from the HASTECS project [53, 54], which provides 2025 and 2035 targets. Values of $5\ kW/kg$ for generators and $15\ kW/kg$ for inverters are considered. It is assumed that these values include component cooling for generators but not for inverters. As a consequence, an additional thermal management system is required for the cooling of inverters and is presented in the following section. Efficiencies of 0.96 and 0.98 are taken for generators and inverters respectively. For power distribution, cables are studied assuming an efficiency of 1. The cable mass is obtained using maximum current constraint and linear mass coefficient. AWG 12 cables are considered with a maximum current of $13.2\ A$ according to the American Wire Gauge (AWG) table. Knowing the required power for a system and an assumed voltage of $230\ VAC$ on the aircraft, a number of wires to respect the maximum current can be estimated taking into account the feasibility of wiring. As a consequence, the cable mass can be found using a maximum linear mass of $87\ g/m$ from MLB Nexans reference cables [55].

4.3.2 Thermal management systems

Different solutions for thermal management are available in order to cool aircraft electric systems [22, 56]. For the aircraft studied in this paper, a thermal management system is only required for power inverters. Indeed, it is assumed that power generators have an independent cooling system based on fuel. Moreover, ECS electric motor models include a cooling part. Finally, cables do not require cooling because the natural convection is sufficient.
Only a few thermal management systems are considered in this paper:

- Air inlet system: outside air, through air inlets, is directly blown on the components to cool;
- Air-air heat exchanger system: local airframe air is blown by an electric fan on the components to cool using an air-air heat exchanger to reject the heat;
- Air-source heat pump system: a refrigerant fluid cools hot components using heat exchangers and a compressor.

These different systems are modeled and compared in [57]. The models used in this paper are the same than in [57], except for the reference mass of the heat pump system which has been updated with industrial data. The Honeywell Micro Vapor Cycle System can provide $20\ kW$ for a system mass of around $64\ kg$ including structural frame [58].
A comparison between the systems is made in terms of induced aircraft fuel consumption, based on models in [57] and models given in section 5.1. Indeed, depending on the amount of heat to dissipate and on the use of the system, the most efficient solution is not the same. Figure 4 gives the additional aircraft fuel consumption due to the different systems for different heat losses to dissipate in the case of a single-aisle aircraft like the CeRAS. Figure 4a represents a case where the thermal management system is used permanently while Figure 4b represents a case where the system is used intermittently (only 5% of the flight duration).

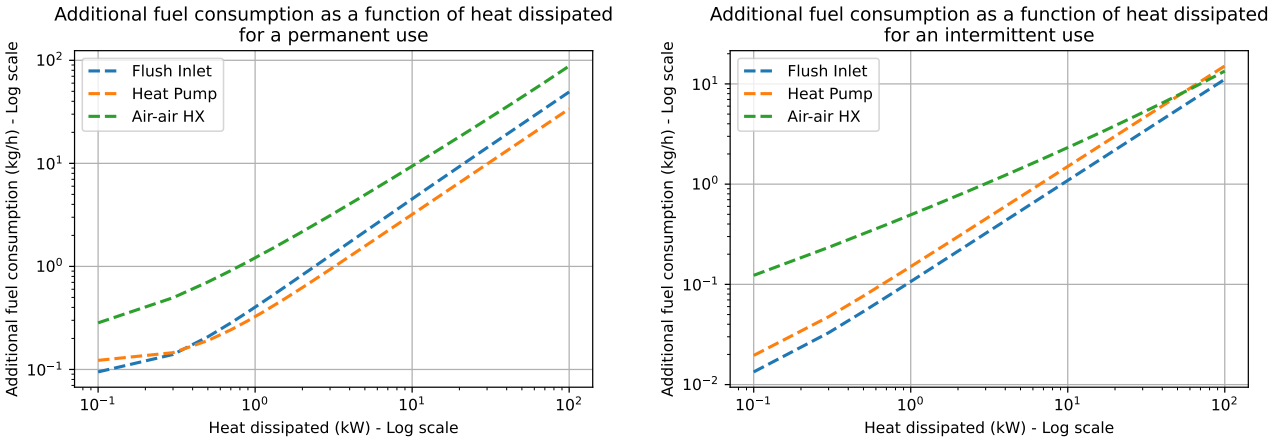

(a) Permanent use

(b) Intermittent use

Figure 4 – Aircraft fuel consumption due to different thermal management systems.

It is interesting to note that the heat pump system is more fuel efficient in permanent use than the system based on air inlets. However, for intermittent use of the thermal management system, the air inlet system is more interesting. Indeed, the heat pump system is heavier than the one based on air inlets. In case of low use, the thermal management system is not active most of the time and the mass has a greater impact on the average consumption. Lastly, the system based on air-air heat exchanger is less interesting in terms of induced fuel consumption.
As a consequence, air inlet system is considered in this paper for cooling power inverters. Indeed, in addition to the fact that air inlet system is the simplest solution, IPS requires an intermittent use and ECS is mainly used for nominal operations without reaching the maximum power. Specific models for air inlets are given in [57] for estimating their mass and additional drag.

5. Sizing and optimization of the aircraft architecture

In this section, the aircraft architecture is sized, optimized and analyzed. The first section provides a model for evaluating the impact of a system on the aircraft fuel consumption. Then, the sizing of the aircraft is performed using the previous models and FAST-OAD for solving the multidisciplinary design and analysis process. Optimizations are also achieved for different cost functions considering the aspect ratio as variable. In a last step, reduced payload and range are assumed for the aircraft sizing and a specific payload-range diagram is performed for comparing the results.
For simplicity's sake, in the following, aircraft architectures studied in the framework of this work will be called BEITA for "Bleedless and Efficient Incremental Technologies Aircraft". A number for specifying the aspect ratio of the aircraft is added. For instance, BEITA-10 has an aspect ratio of 10.

5.1 Impact of a system on an aircraft

Adding an electrical system in an aircraft increases fuel consumption. This increase can have three different causes: an increase in mass, an additional drag or an additional electrical consumption.
A solution to quickly and separately assess the additional mass of fuel ΔM_F due to a new system is to use equation (7) adapted from [59]. This model is for instance used for comparing the different thermal management systems [57].

$$\Delta M_F = \underbrace{\Delta M_S \left(e^{\frac{ctg}{f}} - 1\right)}_{Mass} + \underbrace{\Delta D_S \frac{f}{g}\left(e^{\frac{ctg}{f}} - 1\right)}_{Drag} + \underbrace{\frac{\kappa}{3600}\frac{\Delta P_S}{\eta_e}\frac{f}{cg}\left(e^{\frac{ctg}{f}} - 1\right)}_{Electric} \tag{7}$$

where ΔM_S is the mass of the system, ΔD_S the additional drag due to the system, ΔP_S the additional electrical power which must be consumed, f the lift-to-drag ratio, c the specific fuel consumption, g the acceleration of terrestrial gravity, t the duration of the flight phase, η_e the efficiency of electric generators (on the turbofan) and κ a coefficient giving the fuel mass flow rate for generating power.
This method is integrated into FAST-OAD in order to estimate the mean fuel consumption due to drag and electric power. However, the mass term of equation (7) is not used during the aircraft sizing because a mass sizing loop is already taken into account in FAST-OAD.

5.2 Sizing of the aircraft

The previous models and parameters have been integrated in FAST-OAD in order to size a new aircraft architecture. The results are given in this section considering an aspect ratio of 9.5 (number rounded to the tenth) and all the geometrical characteristics assumed for CeRAS.
Table 3 provides the CeRAS data and the results obtained for BEITA-9.5. Despite its higher OWE, BEITA-9.5 allows a fuel consumption reduction of 15% compared to CeRAS for the sizing mission.

Table 3 – Aircraft comparison between CeRAS and BEITA-9.5 on the sizing mission.

Parameter	CeRAS	BEITA-9.5	Unit
Maximum Take-Off Weight (MTOW)	77.0	77.5	t
Operating Weight Empty (OWE)	42.1	44.6	t
Wing area	122.4	126.8	m^2
Fuel consumption for sizing mission	15.0	12.8	t
CO_2 emissions per RPK (direct emissions)	68	58	g/RPK
CO_2 emissions per RPK (all life cycle)	79	67	g/RPK

In addition to the global aircraft characteristics, the impact of the different systems studied in this paper is given. First, the average use of the ECS generates a mean drag of $200\ N$ and consumes a mean electric power of around $190\ kW$. For the IPS, which is assumed to be used 2% of the flight in average, the maximum electric power is $68\ kW$, resulting in coefficients of performance of $2.6\ kW/m^2$ for wing and $3.9\ kW/m^2$ for nacelles. Excluding the mass impact, the bleedless systems and the additional systems due to electrification are responsible of 3.9% of the fuel consumption during the mission. Lastly, the total mass of these systems is $1660\ kg$, of which 90% for ECS (including cabin distribution ducts) and 5% for IPS.

The sizing of BEITA-9.5 allows estimating its fuel consumption on the design and study missions considering 150 passengers for a payload of $13.6\ t$. For $2750\ NM$, the total fuel consumption is $13.4\ t$ and direct emissions are $55\ gCO_2/RPK$. Similarly, for $800\ NM$, the total fuel consumption is $4.4\ t$ and direct emissions are $63\ gCO_2/RPK$. Therefore, this represents a difference of 13% in terms of CO_2 emissions per RPK between the two missions.

5.3 Optimizations for different objectives

The objective of this section is to optimize the aircraft architecture considering the aspect ratio as a design variable. Two optimization objectives (to minimize) are studied in this paper: the aircraft mass through its MTOW and the aircraft fuel consumption through its fuel mass for the design mission. Other objectives such as operating costs could be studied.

By minimizing the MTOW, an optimal aspect ratio of 8.3 is found. For the optimization on fuel consumption, an aspect ratio of 18.6 is found. However, results are only illustrative for high aspect ratios, because FAST-OAD does not include models for required structural changes like strut-braced wings. To illustrate the architectures obtained, Figure 5 provides comparisons of geometry and mass.

As a consequence, minimizing MTOW and minimizing fuel consumption do not lead to the same results. Indeed, in this case, increasing the aspect ratio allows improving the aerodynamic performance despite the increased mass. It is interesting to note that, for an aircraft, reducing its climate and environmental impact is equivalent to reducing its fuel consumption [35].

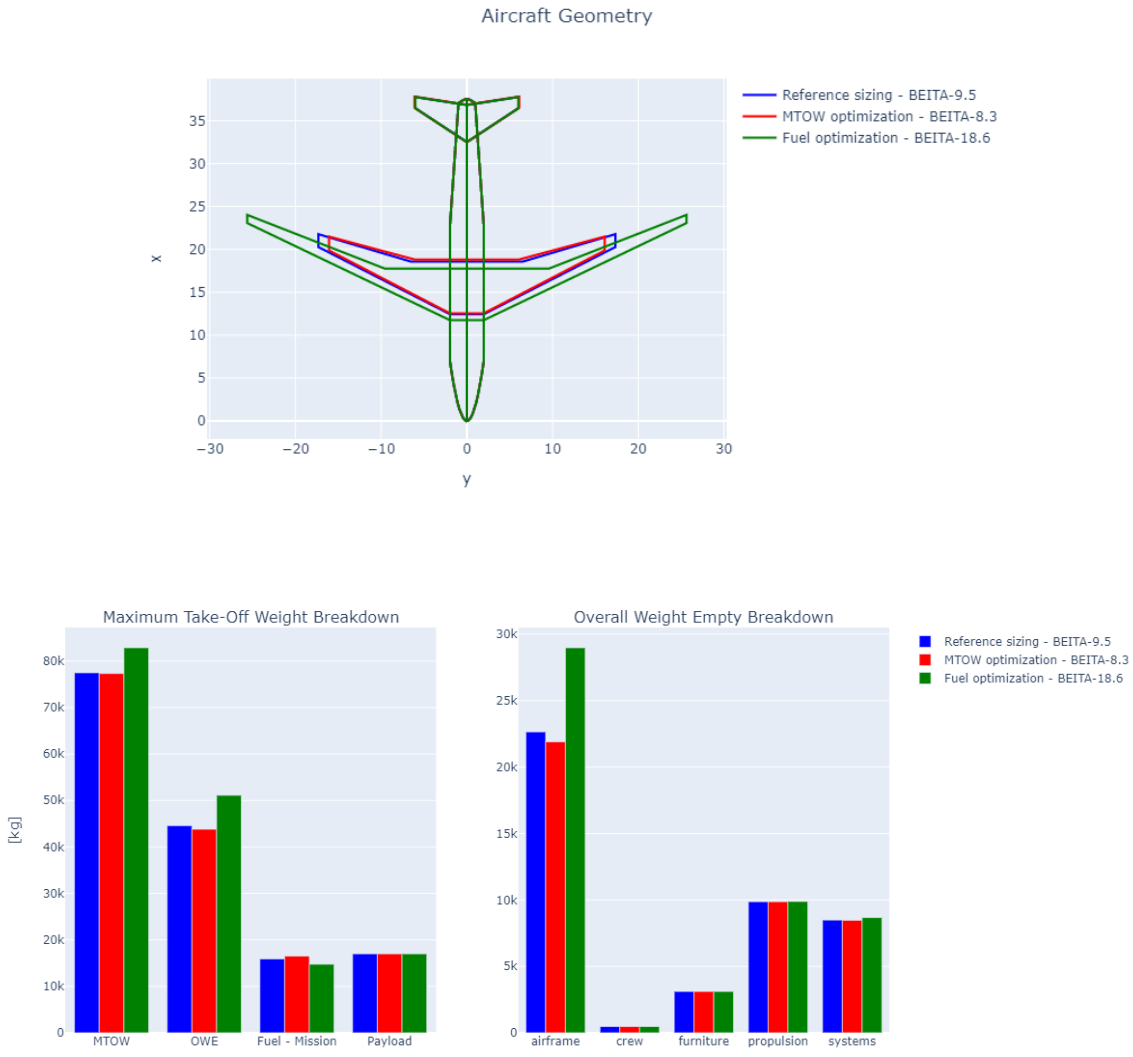

Figure 5 – Geometry (top) and mass breakdown (bottom) of the reference and optimized aircraft.

5.4 Impact of payload and range reduction using payload-range diagram

To complete these analyses, a study of the impact of payload and range reduction on the sizing of the aircraft is carried out. Indeed, aircraft are oversized for flexibility reasons (payload and range adaptability, fewer different aircraft, cost reduction...) and are often used in flight conditions with a reduced payload or range [60].

For instance, the aircraft is sized using the initial aspect ratio of 9.5 and considering the study mission, with the study payload of $13.6\ t$ (with a maximum payload of $15\ t$) and the reduced range of $800\ NM$. The engine is kept as it is but it is also possible to size a new one to improve efficiency. The aircraft obtained has an OWE of $40.9\ t$, which is less than the aircraft obtained in the previous section. For this study mission, the new sizing allows to marginally reduce fuel consumption by 4%, which is consistent with literature [61]. However, this new architecture cannot achieve higher performance in terms of range and payload, which induces a reduced flexibility of use for the operator.

An easy way to compare aircraft performance is to plot their respective payload-range diagrams. The results are given in Figure 6. In addition to the operating limits shown through the black line, the performance in terms of fuel consumption per payload and per range is provided on a colored scale. For instance, for the aircraft sized for the initial TLARs, for a mission of $3000\ NM$ with a payload of $15\ t$, the fuel consumption per payload and per range is $1.2 \cdot 10^{-4}\ kg_{fuel}/kg_{payload}/km$. It is interesting to note the performance drop for ranges below $1000\ NM$.

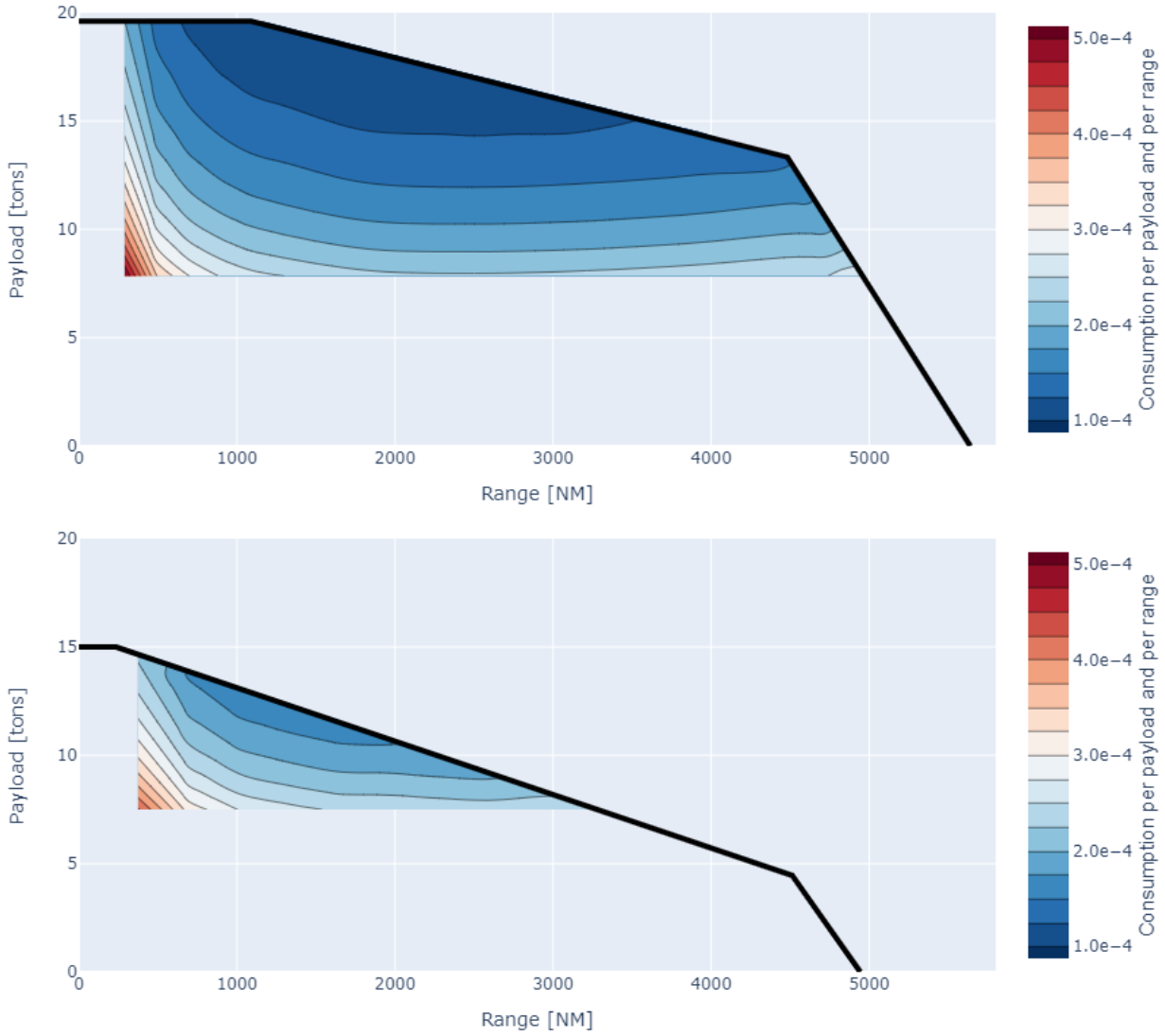

Figure 6 – Payload-range diagrams for the aircraft sized for initial (top) and study (bottom) TLARs.

6. Conclusions

In this paper, the sizing of BEITA, a short-medium range aircraft available by 2025-2030, is achieved. This aircraft is based on more efficient UHBR engines, improvements in aerodynamics and structure, and bleedless systems including induced electric systems (power generation and distribution, thermal management). Different optimizations and analyses are achieved to assess BEITA characteristics and performance.

In terms of modeling, the approach has been based on the development of simplified models adapted for use in preliminary aircraft design. A rubber engine has been used to estimate the performance of a simplified UHBR engine whereas aerodynamics and structure have been taken into account using aspect ratio and correction factors respectively. For bleedless aircraft systems, energy methods have been used in order to estimate the power requirements and specific models have been developed for estimating the mass of these systems. Their integration requires adding systems, for electric power generation and distribution and for thermal management, which have also been modeled. Finally, these models have been integrated into FAST-OAD, an overall aircraft design platform, for sizing the aircraft architecture according to different assumptions.

Different analyses have been carried out in this paper. First, a comparison between CeRAS and BEITA has been achieved and has showed a fuel consumption reduction of 15%. Then, BEITA has been optimized using the aspect ratio as design variable and considering different cost functions as objective. Different optimal aspect ratios have been found between minimizing aircraft mass and fuel consumption. Finally, a sizing for reduced payload and range has been studied using payload-range diagrams and leads to marginal gains in fuel consumption, limited by the reduced flexibility of aircraft use.

This work could be complemented by additional studies. First, additional models could be developed to incorporate incremental improvements not covered in this paper such as the replacement of hydraulic systems. Surrogate models of airframe systems or other disciplines could be developed to be more easily integrated into overall aircraft design platforms. Moreover, the methodology used could be applied to more innovative architectures in terms of structures, propulsion or even fuel used such as hydrogen. This would require the development of specific models to be integrated into FAST-OAD. Secondly, a better integration of the systems into FAST-OAD could be done by assessing the consumption of the systems step by step and not on average for the flight. Lastly, this method could be used to optimize future aircraft TLARs using payload-range analyses. The estimates obtained for the studied architectures could be used to help define prospective scenarios based on technological gains for sustainable air transport.

7. Acknowledgements

The authors would like to thank Robbe Creelle and Martin Dierge for their help with FAST-OAD post-processing tools.

8. Supplementary materials

FAST-OAD is available online at `https://github.com/fast-aircraft-design/FAST-OAD`.

9. Contact Author Email Address

mailto: thomas.planes@isae-supaero.fr

10. Copyright Statement

References

[1] Lee, D. S., Fahey, D., Skowron, A., Allen, M., Burkhardt, U., Chen, Q., Doherty, S., Freeman, S., Forster, P., Fuglestvedt, J., and others„ "The contribution of global aviation to anthropogenic climate forcing for 2000 to 2018," *Atmospheric Environment*, vol. 244, p. 117834, 2021.

[2] Planès, T., Delbecq, S., Pommier-Budinger, V., and Bénard, E., "Simulation and evaluation of sustainable climate trajectories for aviation," *Journal of Environmental Management*, vol. 295, p. 113079, 2021.

[3] Grewe, V., Rao, A. G., Grönstedt, T., Xisto, C., Linke, F., Melkert, J., Middel, J., Ohlenforst, B., Blakey, S., Christie, S., and others„ "Evaluating the climate impact of aviation emission scenarios towards the paris agreement including covid-19 effects," *Nature Communications*, vol. 12, no. 1, pp. 1–10, 2021.

[4] Klöwer, M., Allen, M., Lee, D., Proud, S., Gallagher, L., and Skowron, A., "Quantifying aviation's contribution to global warming," *Environmental Research Letters*, vol. 16, no. 10, p. 104027, 2021.

[5] Delbecq, S., Fontane, J., Gourdain, N., Mugnier, H., Planes, T., and Simatos, F., "ISAE-SUPAERO aviation and climate: a literature review," 2022.

[6] Moua, L., Roa, J., Xie, Y., and Maxwell, D., "Critical review of advancements and challenges of all-electric aviation," in *International Conference on Transportation and Development 2020*, pp. 48–59, American Society of Civil Engineers Reston, VA, 2020.

[7] Khandelwal, B., Karakurt, A., Sekaran, P. R., Sethi, V., and Singh, R., "Hydrogen powered aircraft: The future of air transport," *Progress in Aerospace Sciences*, vol. 60, pp. 45–59, 2013.

[8] Staples, M. D., Malina, R., Suresh, P., Hileman, J. I., and Barrett, S. R., "Aviation co2 emissions reductions from the use of alternative jet fuels," *Energy Policy*, vol. 114, pp. 342–354, 2018.

[9] De Jong, S., Antonissen, K., Hoefnagels, R., Lonza, L., Wang, M., Faaij, A., and Junginger, M., "Life-cycle analysis of greenhouse gas emissions from renewable jet fuel production," *Biotechnology for biofuels*, vol. 10, no. 1, pp. 1–18, 2017.

[10] Ueckerdt, F., Bauer, C., Dirnaichner, A., Everall, J., Sacchi, R., and Luderer, G., "Potential and risks of hydrogen-based e-fuels in climate change mitigation," *Nature Climate Change*, vol. 11, no. 5, pp. 384–393, 2021.

[11] Lee, J. J., "Can we accelerate the improvement of energy efficiency in aircraft systems?," *Energy conversion and management*, vol. 51, no. 1, pp. 189–196, 2010.

[12] AbdElhafez, A. and Forsyth, A., "A review of more-electric aircraft," in *International Conference on Aerospace Sciences and Aviation Technology*, vol. 13, pp. 1–13, The Military Technical College, 2009.

[13] Tfaily, A. and Kokkolaras, M., "Integrating air systems in aircraft multidisciplinary design optimization," in *2018 Multidisciplinary Analysis and Optimization Conference*, p. 3742, 2018.

[14] Chakraborty, I., Mavris, D. N., Emeneth, M., and Schneegans, A., "An integrated approach to vehicle and subsystem sizing and analysis for novel subsystem architectures," *Proceedings of the Institution of Mechanical Engineers, Part G: Journal of Aerospace Engineering*, vol. 230, no. 3, pp. 496–514, 2016.

[15] Chakraborty, I., Trawick, D., Mavris, D., Emeneth, M., and Schneegans, A., "Integrating subsystem architecture sizing and analysis into the conceptual aircraft design phase," in *4th Symposium in Collaboration in Aircraft Design*, 2014.

[16] Crabé, C., Joksimovic, A., Benichou, E., and Carbonneau, X., "A methodology to evaluate electric environmental control system impact on aircraft drag and mission performance," in *AIAA Aviation 2019 Forum*, p. 2803, 2019.

[17] Shinkafi, A. and Lawson, C., "Enhanced method of conceptual sizing of aircraft electro-thermal de-icing system," *International Journal of Mechanical, Aerospace, Industrial and Mechatronics Engineering*, vol. 8, no. 6, pp. 1069–1076, 2014.

[18] Budinger, M., Pommier-Budinger, V., Reysset, A., and Palanque, V., "Electromechanical resonant ice protection systems: Energetic and power considerations," *AIAA Journal*, pp. 1–13, 2021.

[19] Palanque, V., Budinger, M., Pommier-Budinger, V., Bennani, L., and Delsart, D., "Electro-mechanical resonant ice protection systems: Power requirements for fractures initiation and propagation," in *AIAA Aviation 2021 Forum*, p. 2651, 2021.

[20] Thomas, S. K., Cassoni, R. P., and MacArthur, C. D., "Aircraft anti-icing and de-icing techniques and modeling," *Journal of aircraft*, vol. 33, no. 5, pp. 841–854, 1996.

[21] Gent, R. W., "Ice detection and protection," *Encyclopedia of Aerospace Engineering*, 2010.

[22] van Heerden, A. S., Judt, D. M., Jafari, S., Lawson, C. P., Nikolaidis, T., and Bosak, D., "Aircraft thermal management: Practices, technology, system architectures, future challenges, and opportunities," *Progress in Aerospace Sciences*, vol. 128, p. 100767, 2022.

[23] Palladino, V., Jordan, A., Bartoli, N., Schmollgruber, P., Pommier-Budinger, V., and Benard, E., "Pre-

liminary studies of a regional aircraft with hydrogen-based hybrid propulsion," in *AIAA AVIATION 2021 FORUM*, p. 2411, 2021.

[24] Riboldi, C. E. and Gualdoni, F., "An integrated approach to the preliminary weight sizing of small electric aircraft," *Aerospace Science and Technology*, vol. 58, pp. 134–149, 2016.

[25] Riboldi, C. E., Gualdoni, F., and Trainelli, L., "Preliminary weight sizing of light pure-electric and hybrid-electric aircraft," *Transportation Research Procedia*, vol. 29, pp. 376–389, 2018.

[26] Epstein, A. H. and O'Flarity, S. M., "Considerations for reducing aviation's co 2 with aircraft electric propulsion," *Journal of Propulsion and Power*, vol. 35, no. 3, pp. 572–582, 2019.

[27] Gnadt, A. R., Speth, R. L., Sabnis, J. S., and Barrett, S. R., "Technical and environmental assessment of all-electric 180-passenger commercial aircraft," *Progress in Aerospace Sciences*, vol. 105, pp. 1–30, 2019.

[28] Abbas, A., De Vicente, J., and Valero, E., "Aerodynamic technologies to improve aircraft performance," *Aerospace Science and Technology*, vol. 28, no. 1, pp. 100–132, 2013.

[29] Welstead, J. and Felder, J. L., "Conceptual design of a single-aisle turboelectric commercial transport with fuselage boundary layer ingestion," in *54th AIAA aerospace sciences meeting*, p. 1027, 2016.

[30] Perez, R., Liu, H., and Behdinan, K., "Evaluation of multidisciplinary optimization approaches for aircraft conceptual design," in *10th AIAA/ISSMO multidisciplinary analysis and optimization conference*, p. 4537, 2004.

[31] Martins, J. R. and Lambe, A. B., "Multidisciplinary design optimization: a survey of architectures," *AIAA journal*, vol. 51, no. 9, pp. 2049–2075, 2013.

[32] Delbecq, S., Budinger, M., and Reysset, A., "Benchmarking of monolithic mdo formulations and derivative computation techniques using openmdao," *Structural and Multidisciplinary Optimization*, vol. 62, no. 2, pp. 645–666, 2020.

[33] Gray, J. S., Hwang, J. T., Martins, J. R. R. A., Moore, K. T., and Naylor, B. A., "OpenMDAO: an open-source framework for multidisciplinary design, analysis, and optimization," *Structural and Multidisciplinary Optimization*, vol. 59, pp. 1075–1104, Apr. 2019.

[34] David, C., Delbecq, S., Defoort, S., Schmollgruber, P., Benard, E., and Pommier-Budinger, V., "From fast to fast-oad: An open source framework for rapid overall aircraft design," in *IOP Conference Series: Materials Science and Engineering*, vol. 1024, p. 012062, IOP Publishing, 2021.

[35] Fabre, A., Planès, T., Delbecq, S., Budinger, V., and Lafforgue, G., "Life cycle assessment models for overall aircraft design," in *AIAA SCITECH 2022 Forum*, p. 1028, 2022.

[36] Huijbregts, M. A., Steinmann, Z. J., Elshout, P. M., Stam, G., Verones, F., Vieira, M., Zijp, M., Hollander, A., and van Zelm, R., "Recipe2016: a harmonised life cycle impact assessment method at midpoint and endpoint level," *The International Journal of Life Cycle Assessment*, vol. 22, no. 2, pp. 138–147, 2017.

[37] Dahlmann, K., Grewe, V., Matthes, S., and Yamashita, H., "Climate assessment of single flights: Deduction of route specific equivalent co2 emissions," *International Journal of Sustainable Transportation*, pp. 1–12, 2021.

[38] Delbecq, S., *Knowledge-based multidisciplinary sizing and optimization of embedded mechatronic systems-application to aerospace electro-mechanical actuation systems*. PhD thesis, Toulouse, INSA, 2018.

[39] Risse, K., Schäfer, K., Schültke, F., and Stumpf, E., "Central reference aircraft data system (ceras) for research community," *CEAS Aeronautical Journal*, vol. 7, no. 1, pp. 121–133, 2016.

[40] Sanchez, F. and Delbecq, S., "Surrogate modeling technique for the conceptual and preliminary design of embedded actuation systems and components," in *International congress of the aeronautical sciences*, 2016.

[41] Giesecke, D., Lehmler, M., Friedrichs, J., Blinstrub, J., Bertsch, L., and Heinze, W., "Evaluation of ultra-high bypass ratio engines for an over-wing aircraft configuration," *Journal of the Global Power and Propulsion Society*, vol. 2, pp. 493–515, 2018.

[42] Roux, É., "Pour une approche analytique de la dynamique du vol," *These, SUPAERO-ONERA*, 2005.

[43] Incropera, F. and DeWitt, D., "Fundamentals of heat transfer 1wiley," *New York*, vol. 19852, p. 8, 1990.

[44] Wolf, D., *Das CORDIER-Diagramm unter besonderer Berücksichtigung der axialen Turboarbeitsmaschine*. na, 2009.

[45] Budinger, M., Liscouët, J., Hospital, F., and Maré, J., "Estimation models for the preliminary design of electromechanical actuators," *Proceedings of the Institution of Mechanical Engineers, Part G: Journal of Aerospace Engineering*, vol. 226, no. 3, pp. 243–259, 2012.

[46] Sinnett, M., "787 no-bleed systems: saving fuel and enhancing operational efficiencies," *Aero Quarterly*, vol. 18, pp. 6–11, 2007.

[47] SAE International„ *SAE Aerospace Applied Thermodynamics Manual*. Society of automotive engineers, 1969.

[48] Al-Khalil, K., Horvath, C., Miller, D., Wright, W., Al-Khalil, K., Horvath, C., Miller, D., and Wright, W., "Validation of nasa thermal ice protection computer codes. iii-the validation of antice," in *35th Aerospace sciences meeting and exhibit*, p. 51, 1997.

[49] Meier, O. and Scholz, D., "A handbook method for the estimation of power requirements for electrical de-icing systems," *DLRK, Hamburg*, vol. 31, 2010.

[50] Heinrich, A., Ross, R., Zumwalt, G., Provorse, J., and Padmanabhan, V., "Aircraft icing handbook. volume 2," tech. rep., GATES LEARJET CORP WICHITA KS, 1991.

[51] Shen, X., Guo, Q., Lin, G., Zeng, Y., and Hu, Z., "Study on loose-coupling methods for aircraft thermal anti-icing system," *Energies*, vol. 13, no. 6, p. 1463, 2020.

[52] Li, R., Xu, W., and Zhang, D., "Impacts of thermal and mechanical cycles on electro-thermal anti-icing system of cfrp laminates embedding sprayable metal film," *Materials*, vol. 14, no. 7, p. 1589, 2021.

[53] Roboam, X., "Hastecs," in *More Electric Aircraft*, 2021.

[54] Roboam, X., Touhami, S., Erroui, N., Zeaiter, A., Accorinti, F., Collin, P., and Pettes-Duler, M., "Hastecs: Hybrid aircraft: research on thermal and electric components and systems," 2021.

[55] Nexans„ "Designed for general purpose aircraft wiring applications," 2015. https://www.direct.fr/245000-fil-aeronautique-mlb22.html.

[56] Adler, E. J., Brelje, B. J., and Martins, J. R., "Thermal management system optimization for a parallel hybrid aircraft considering mission fuel burn," *Aerospace*, vol. 9, no. 5, p. 243, 2022.

[57] Planès, T., Habrard, V., Delbecq, S., Pommier-Budinger, V., and Benard, E., "Thermal management system models for overall aircraft design," in *AIAA AVIATION 2021 FORUM*, p. 2428, 2021.

[58] Ainonline„ "Honeywell develops a/c system for future flyers," 2020. https://www.ainonline.com/aviation-news/aerospace/2020-06-22/honeywell-develops-c-system-future-flyers.

[59] Moir, I. and Seabridge, A., *Design and development of aircraft systems*, vol. 67. John Wiley & Sons, 2012.

[60] Husemann, M., Schäfer, K., and Stumpf, E., "Flexibility within flight operations as an evaluation criterion for preliminary aircraft design," *Journal of Air Transport Management*, vol. 71, pp. 201–214, 2018.

[61] Kenway, G., Henderson, R., Hicken, J., Kuntawala, N., Zingg, D., Martins, J. R., and McKeand, R., "Reducing aviation's environmental impact through large aircraft for short ranges," in *48th AIAA Aerospace Sciences Meeting Including the New Horizons Forum and Aerospace Exposition*, p. 1015, 2010.